SYNTHESIS OF IRON OXIDE NANOPARTICLES FROM COLONIAL TUNICATE

ECTEINASCIDIA VENUI

S. Sankaravadivu, 10176, PG and Research Department of Chemistry, V.O.C College, Thoothukudi
Dr. R. Jothibai Margret, Associate Professor, Department of Chemistry, Pope's College, Sawyerpuram
Dr. V.K. Meenakshi, Associate Professor (Retired), Department of Zoology,
A.P.C. Mahalaxmi College for women, Thoothukudi
Manonmaniam Sundaranar University, Abishekapatti, Tirunelveli – 627 012.

Abstract: ***Iron oxide nanoparticles (NPs) are gaining importance for their uses in environmental remediation technologies. In the present investigation FeO NPs were synthesized by colonial tunicate Ecteinascidia venui. FeO NPs were generated by reaction of ferric chloride ($FeCl_3$) solution with tunicate extracts. The reductants present in the tunicate extracts act as reducing and stabilizing agent. Synthesized NPs were characterized using FTIR, UV-Vis absorption spectrophotometer, XRD and SEM. FT-IR measurement was carried out to identify the possible molecules like CO, CH, OH band. UV-Vis absorption shows a characteristic absorption peak of iron oxide NPs in the range of 190-250 nm. From the XRD, it was found that the average particle size of magnetite NPs was found to be 111 plane. SEM image shows agglomerated structure. AFM and Redox potential show the nature of iron oxide NPs and applications of iron oxide NPs predicts the better antioxidant activity. This biosynthetic approach is cost effective, eco-friendly and has promising valuable applications in medicine.***

Keywords: Ecteinascidia venui, SEM, Tunicates, XRD

I. INTRODUCTION

The development of nanotechnology is not only for their fundamental scientific interest, but also for offering many technological solutions. Oxides of iron are available widely in nature in different phases (Cornell and Schwertmann, 2014). Additionally, iron oxides have attracted a great deal of attention among specialists because of their multivalent oxidation states (Lisiecki *et al*.,1996), a large set of possible polymorphisms (Benz *et al*., 1998) and especially at the nano scale, their characteristic structural changes (Cornell and Schwertmann, 2014). These materials have a considerable potential to be applied as sensors, in catalysis (Weiss *et al*., 2002), high-density magnetic recording media (Koksharov, 2001), targeted drug delivery in clinical trials (Kim *et al*., 2001), and as substrates in cancer treatment methods (Jordan *et al*., 1999). Iron oxides are relatively inert, non-toxic, and present in living organisms (Cornell and Schwertmann, 2014). Over the last few years, various synthetic methods have been developed to produce iron NPs, modify the NPs surface properties and enhance its efficiency for field delivery and reactions (Xu *et al*., 2012, Nadagouda *et al*., 2010, Sun *et al*., 2006 and Li *et al*., 2006). The most widely used method for environmental purposes is the borohydrate reduction of Fe(II) or Fe(III) ions in aqueous media. The present study deals with biosynthesis, characterisation and applications of stable iron oxide NPs from *Ecteinascidia venui* extract.

II. MATERIALS AND METHODS

2.1 Preparation of sample from tunicates

Samples of *Ecteinascidia venui* were collected and epibionts adhering to the surface of tunicates were carefully removed. The specimen were washed several times with sterile sea water and dried separately under shade. The dried animals were homogenized to get a coarse powder which was stored in separate air tight container.

2.2 Synthesis of iron oxide nanoparticles

Iron oxide NPs were synthesised by the standard method (Balamurugan *et al.*, 2014). In the synthesis of iron oxide NPs, ethanolic extract of *Ecteinascidia venui* was used in order to reduce and cap the Fe ions. 20 ml of the extract was dripped slowly into the aqueous solution of $FeCl_3$ with constant stirring at room temperature with normal atmosphere pressure. After adding the extract into $FeCl_3$ solutions within 3 mins a visible color change was observed, the yellow color aqueous solution of $FeCl_3$ turned to greenish black which was dried in a muffle furnace to collect iron oxide NPs. This powder was further used for the characterisation of iron oxide NPs.

2.3 Characterisation of nanoparticles

The above synthesised NPs were characterised by FT-IR, UV, XRD, SEM, AFM and Redox potential.

(i) FT-IR spectral analysis

The FT-IR spectra of iron oxide NPs was determined using a Fourier Transform Infrared Spectrometer (Thermo scientific Nicolet is 5) iD_5 ATR/ Attenuated Total Reflectance) - znse (zinc selenide) Accessory system. One mg of finely powdered nanoparticle was mixed with about 100 mg of dried potassium bromide (IR grade) powder. The mixture was then pressed in a special dye to yield a transparent disc. The disc was then held in the instrument beam for spectroscopic examination and the resulting IR spectrum was recorded.

(ii) UV-Visible spectroscopic studies

The surface Plasmon resonances (SPR) of synthesized NPs have been studied by UV-Vis double-beam bio-spectrophotometer. After the addition of *Ecteinascidia venui* extract into the aqueous solution of $FeCl_3$, the reaction mixture was filled in a glass cuvette of path length 10 mm and spectral analysis has been done in the range of 300 to 700 nm. DI water was used as blank.

(iii) XRD analysis

The phase variety and grain size of synthesized iron oxide NPs were determined by X-ray diffraction spectroscopy (Philips PAN analytical). The synthesized iron oxide nanoparticles were studied with CUKα radiation at voltage of 30 kV and current of 20 MA with scan

rate of 0.030/s. Different phases present in the synthesized samples were determined by X′ pert high score software with search and match facility. Particle size of the prepared samples were determined by using Scherrer′s equation.

(iv) SEM and EDAX analysis

Morphological features of the synthesized iron oxide NPs were studied by Scanning Electron Microscope (JSM-6480 LV). After 24 hrs of the addition of $FeCl_3$ solutions, the SEM slides were prepared by making a smear of the solutions on slides. A thin layer of platinum was coated to make the samples conductive. Then the samples were characterized in the SEM at an accelerating voltage of 20 KV. Inorganic metals present in the samples were identified by EDAX characterisation.

(v) AFM analysis

A thin film of iron oxide NPs were prepared on a silica glass plate by dropping a few drops and allowed to dry at room temperature in the dark (to avoid NPs diameter growth due to temperature and/or light). The deposited film on silica glass plate was then scanned with the Atomic Force Microscopy

(vi) Redox potential

Cyclic voltammograms trace the transfer of electrons during an oxidation-reduction (redox) reaction. The potential of an electrode in solution is linearly cycled from a starting potential to final potential and back to the starting potential. Here, the current is measured as a function of potential. This process, in turn, cycles the redox reaction. Multiple cycles can takes place. The system starts off with an initial potential at which no redox can takes place.

2.4 Applications of nanoparticles

(i) Antioxidant studies

DPPH radical scavenging activity of antioxidant component was carried out by Blois method (Blois, 1958). This method is based on the reduction of DPPH in methanol solution in presence of a hydrogen donating antioxidant due to the formation of the non-radical form DPPH-H. 0.1 mM solution of DPPH in methanol was prepared. 1 ml of this solution was added to 3 ml of various solvent extracts at different concentration (50, 100, 200, 400 and 800 µg/ml). The mixtures were shaken vigorously and allowed to stand at room temperature for 30 minutes. Then the absorbance was measured at 517 nm. A standard was also run with 1 mg of ascorbic acid in 10 ml of water. A blank was prepared with 3 ml of distilled water and all other reagents in the same proportion as used for the experimental tubes.

The capability to scavenge free radical was calculated by using the following formula.

$$\text{Scavenging effect (\% inhibition)} = \frac{A_0 - A_1}{A_0} \times 100$$

A_0 - absorbance of the control reaction

A_1 - absorbance in presence of all the extract samples and standard ascorbic acid.

III. RESULTS AND DISCUSSION

3.1 FT-IR spectral studies of iron oxide nanoparticles

Fig. 1 shows the FT-IR spectrum of prepared iron oxide NPs. It displays three strong bands around 3463.03 cm^{-1} (br), 1637.00 cm^{-1} and 600.42 cm^{-1}. The observed bands are similar to those reported for Fe_2O_3 (Matheswaran, 2014). The vibration bands are 600.42 cm^{-1} (Fe-O str), 1637.00 cm^{-1} (H_2O bending vibration) and a broad peak at 3463.03 cm^{-1} (H_2O str). Presence of organic molecule on the surface of iron oxide NPs has the influence on the FT-IR peaks (Lalitha *et al*., 2013). The broad peak observed around 504.69 cm-1 (Fe-O str) instead of two sharp peaks, may be due to the presence of organic molecule from the extract settled on the surface of iron oxide NPs.

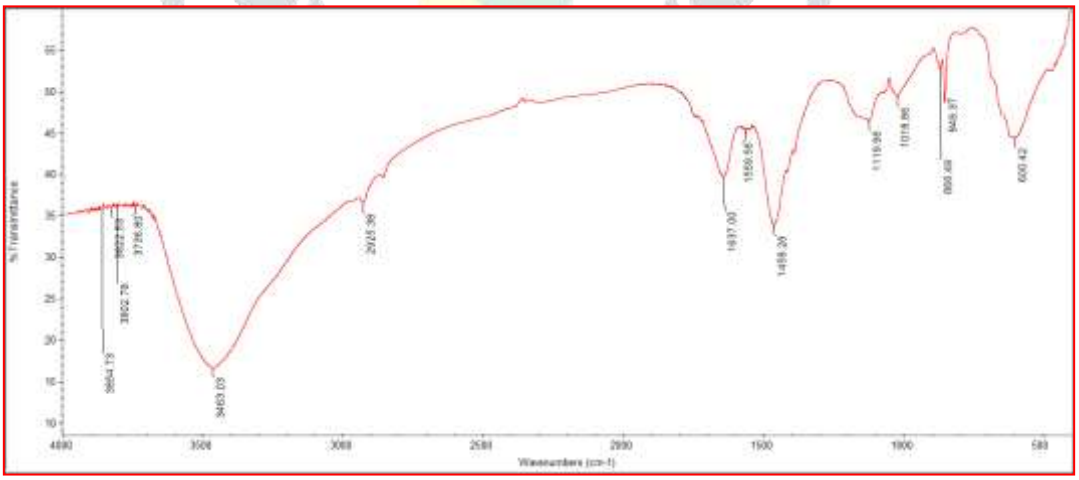

Fig. 1. FT-IR spectrum of iron oxide nanoparticles from *Ecteinascidia venui* extract

3.2 UV-Visible spectroscopic analysis of iron oxide nanoparticles

The bioreduction of Fe+3 in aqueous solutions was monitored by periodic sampling of aliquots of the mixture and subsequently measuring UV–Vis spectra. UV-Vis spectral analysis was done at the range of 250-500 nm. The observed absorption peaks were due to the excitation of surface plasmon vibrations in the iron oxide NPs (250 nm), which are identical to the characteristic UV visible spectrum of metallic iron and it was recorded in fig. 2.

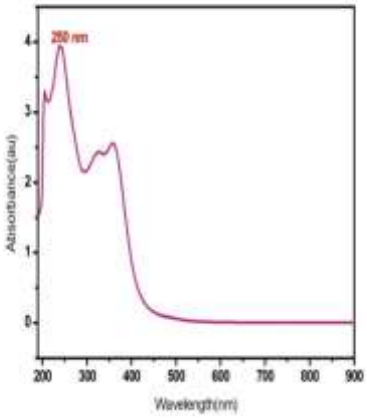

Fig. 2. UV spectrum of iron oxide nanoparticles from *Ecteinascidia venui* extract

3.3 XRD analysis of iron oxide nanoparticles

Fig. 3 shows the XRD pattern of iron oxide NPs prepared by using extract. All the diffraction peaks in this pattern were found to be in good agreement with JCPDF No: 089-2810, which is corresponding to Fe_2O_3 in rhombohedral geometry. The sample showed the major characteristic peaks for prepared crystalline metallic NPs at values of 29.22, 31.9, 34.03, 40.12, 45.67, 56.62, 66.3 and 75.4 corresponding to (111), (002), (012), (112), (22-1), (113), (123), and (410) respectively.

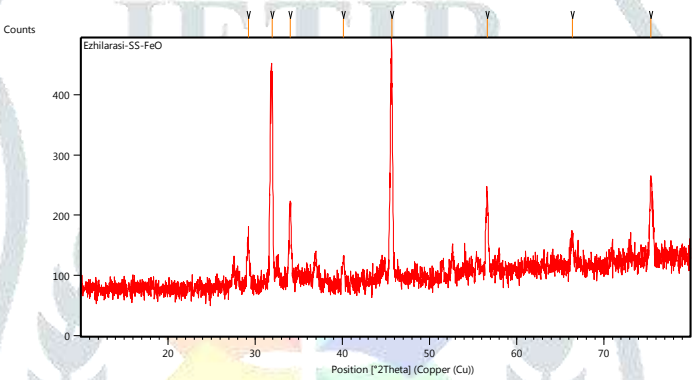

Fig. 3. XRD studies of iron oxide nanoparticles from *Ecteinascidia venui* extract

3.4 SEM and EDAX analysis of iron oxide nanoparticles

Fig. 4 shows the SEM image of Fe_2O_3 NPs prepared from 100 ml of 0.01 M aqueous $FeCl_3$ solutions with the extract. SEM image shows clear morphology of Fe_2O_3 NPs. The SEM also reveals that NPs are agglomerated. The atomic percentages obtained from EDX quantification were 78.98% of O, 8.38% of Fe, and 12.65 % of S. These values could be helpful in reflecting the atomic content on the surface and near surface regions of the NPs in fig. 5.

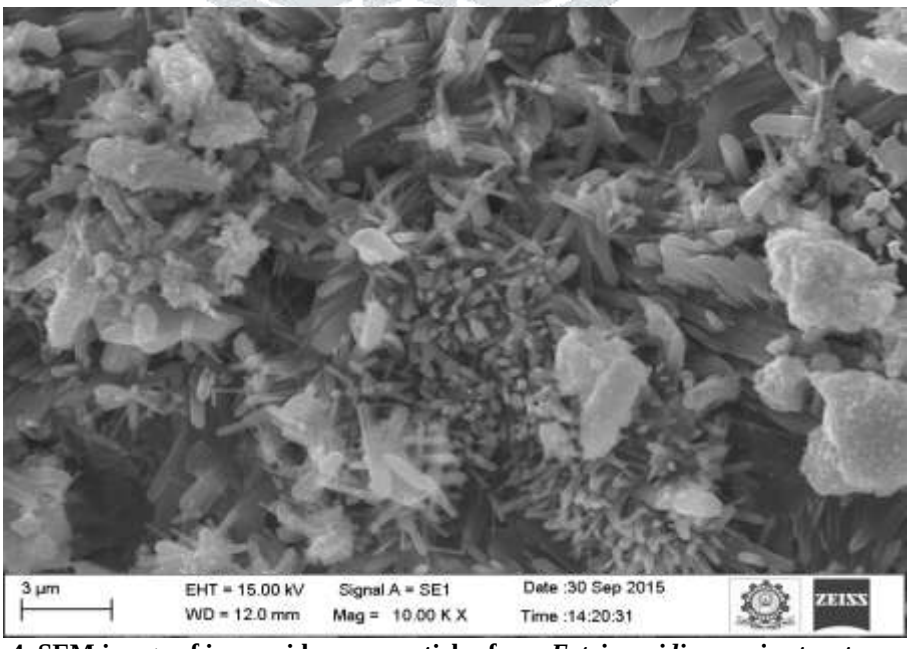

Fig. 4. SEM image of iron oxide nanoparticles from *Ecteinascidia venui* extract

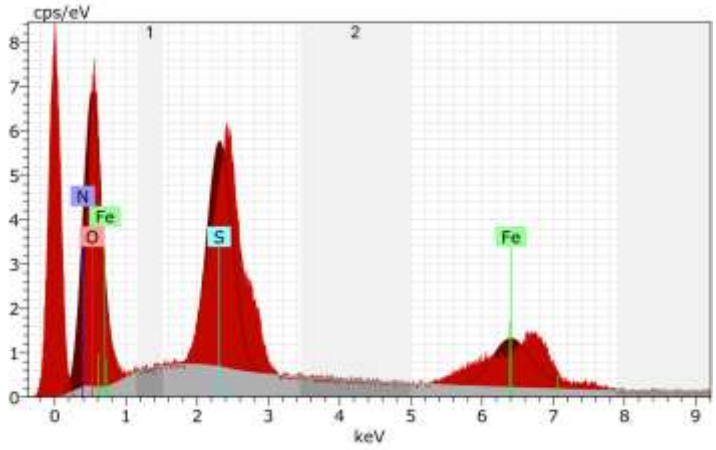

Fig. 5. EDAX image of iron oxide nanoparticles from *Ecteinascidia venue*

3.5 AFM analysis of iron oxide nanoparticles

The micrographs clearly indicate that the formulated iron oxide NPs possess spherical shape and have the calculated size in the range of 1.56 µm within nm range (247nm) in Fig. 6.

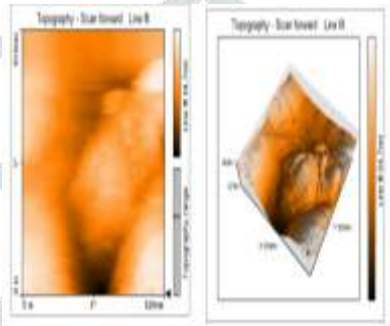

Fig. 6. AFM image of iron oxide nanoparticles from *Ecteinascidia venui*

3.6 Redox potential

Fig. 7, the voltammogram of NPs exhibited one sharp cathodic peak. This behaviour is associated with the electroactive nature of iron oxide NPs.

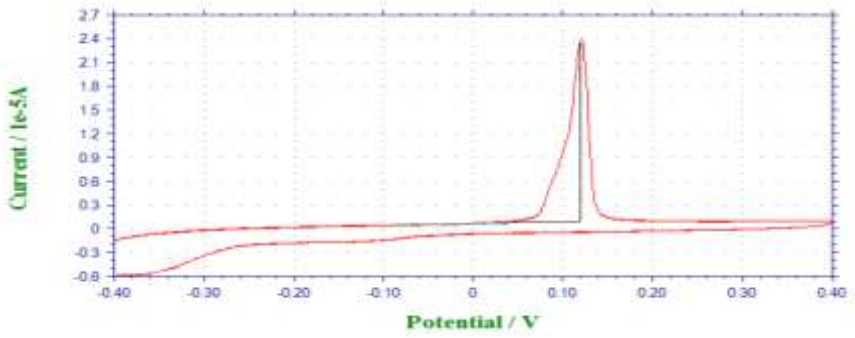

Fig. 7. Redox potential of iron oxide nanopartilces from *Ecteinascidia venui*

3.7 Applications

Antioxidant studies

DPPH radical scavenging activity of petroleum ether, benzene, ethyl acetate, methanol and ethanol extracts of Iron oxide NPs from *Ecteinascidia venui* is presented in table 1. Iron oxide NPs from *Ecteinascidia venui* of different extracts and standard showed maximum percentage inhibition in the following order - petroleum ether (115.21), methanol (97.12), benzene (95.24), ethyl acetate (90.71), ethanol (83.71) and standard (75.15) with IC_{50} values of 54.92, 46.24, 45.26, 40.74, 41.37 and 30.46 µg/ml respectively. Petroleum ether extract of *Ecteinascidia venui* at 800 µg/ml showed significant scavenging activity compared to the standard ascorbic acid.

Table 1. DPPH radical scavenging activity of iron oxide nanoparticles from *Ecteinascidia venui*

Concentration	Different Solvent Extract					
	Petroleum Ether	Benzene	Ethyl Acetate	Methanol	Ethanol	Standard (Ascorbic acid)
50	31.71±0.64	24.17±0.35	29.24±.74	30.41±0.81	21.38±0.54	19.54±0.34
100	53.81±0.61	40.28±0.27	44.34±0.18	48.28±0.14	38.54±0.72	35.59±0.18
200	68.14±0.29	59.91±0.82	71.28±0.35	73.46±0.17	71.28±0.35	48.55±0.36
400	92.28±0.24	80.41±0.41	84.27±0.28	86.21±0.31	84.27±0.28	66.81±0.53

800	115.21±0.14	95.24±0.94	90.71±0.28	97.12±0.46	83.71±0.28	75.15±0.15
IC_{50}	**54.92**	**45.26**	**40.74**	**46.24**	**41.37**	**30.46**

The biological approach of synthesis of iron oxide NPs as described in the present paper appears to be ecofriendly and cost effective alternative to conventional chemical and physical methods and would be suitable for developing large-scale production. This iron oxide NPs may be used in effluent treatment, environmental remediation, biotechnological and biomedical applications.

IV. REFERENCES

[1] Cornell, R.M. and Schwertmann, U. 2014. The Iron Oxides- structure, properties, reactions, occurrences and uses. e-Journal of Surface Science and Nanotechnology, 12: 2.

[2] Lisiecki, I. Billoudet, F. and Pileni, M.P. 1996. Control of the shape and the size of copper metallic properties. Journal of Physical Chemistry, 100(10): 4160-4166.

[3] Benz, M. Van der Kraan, A.M. and Prins, R. 1998. Reduction of aromatic nitrocompounds with hydrazine hydrate in the presence of an Iron oxide hydroxide catalyst - II. Activity, X-ay Diffraction and Mossbauer study of the Iron oxide hydroxide catalyst. Prins, Journal of Applied Catalysis, A 172: 149.

[4] Weiss, W. and Ranke, W. 2002. Surface Chemistry and catalysis on well-defined epitaxial iron oxide layers. Progress in Surface Science, 70(1): 152.

[5] Koksharov, Yu. A. 2001. Electron paramagnetic resonance of ferrite nanoparticles, Journal of Applied Physics, 89: 2293.

[6] Kim, D.K. Zhang, Y. Voit, W. Rao, K.V. Kehr, J. Bjelke, B and Mohamed, M. Superparamagnetic iron oxide nanoparticles for biomedical applications. Scripta. Materialia, 44: 1713-1717.

[7] Jordan, A R. Scholz, P. Wust, H. Fahling, S. and Felix, R. 1999. Magnetic fluid hyperthermia: Cancer treatment with A C magnetic field induced excitation of biocompatible superparamagnetic nanopartcles, Journal of Magnetism and Magnetic Materials, 201: 413.

[8] Xu, P. Zeng, G.M. Huang, D.L. Feng, C.L. Hu, S. Zhao, M.H. Lai, C. Wei, Z. Huang, C. Xie, G.X. and Liu, X. 2012. Incorporating bioaccessbiity into human health risk assessments of heavy metals in urban park soils, Sciience of the Total Environment, 424: 88-96.

[9] Nadagouda, A. B. Castle, R. Murdock, S. Hussain, S.M. and Varma, R.S. 2010. *In vitro* biocompatibility of nanoscale zerovalent iron particles synthesized using tea polyphenols, Green Chemistry, 12: 114.

[10] Sun, Y. Li, X. Cao, J. Zhang, W and Wang, H.P. 2006. Characterization of zerovalent iron nanoparticles. Advances in Colloid and Interface Science, 120: 47.

[11] Li, L. Fan, M. Brown, R.C. and Van Leeuwen, L. 2006. Synthesis, properties, and environmental applications of nanoscale iron based materials: A review. Critical Reviews in Environmental Science and Technology, 36: 405.

[12] Balamurugan, M. and Shanmugam, S. 2014. Synthesis of Iron oxide nanoparticles by using *Eucalyptus globulus* plant extract, e-journal of Surface Science and Nanotechnology, 12: 363-367.

[13] Blois, M.S. 1958. Antioxidant determination by the use of a stable free radical, Nature. A, 26:1199-1200.

[14] Matheswaran, B. 2014. Synthesis of iron oxide nanoparticles by using *Eucalyptus globulus* plant extract, e-journal of Surface Sciences and Nanotechnology, 13: 383-387.

[15] Lalitha, A. Subbaiya, R. and Ponmurugan, P. 2013. Green synthesis of silver nanoparticles from leaf extract: *Azhadirachta indica* and to study its antibacterial and antioxidant property, Interrnational Journal of Current Microbiology and Applied Sciences, 2(60): 228-235.